This is the peer reviewd version of the followng article:

Effect of silicate modulus on the setting, mechanical strength and microstructure of iron-rich aluminosilicate (laterite) based-geopolymer cured at room temperature / Kaze, C.R., Djobo, J.N.Y., Nana, A., Tchakoute, H.K., Kamseu, E., Melo, U.C., Leonelli, C., Rahier, H.. - In: CERAMICS INTERNATIONAL. - ISSN 0272-8842. - 44:17(2018), pp. 21442-21450. [10.1016/j.ceramint.2018.08.205]

Terms of use:

The terms and conditions for the reuse of this version of the manuscript are specified in the publishing policy. For all terms of use and more information see the publisher's website.

09/11/2026 07:28

(Article begins on next page)

Author's Accepted Manuscript

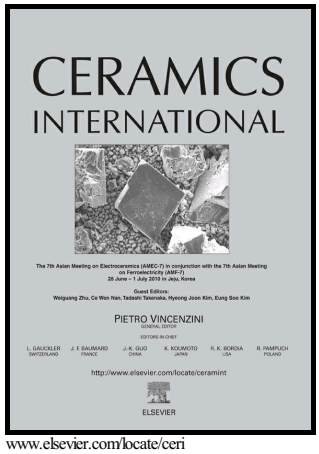

www.elsevier.com/locate/ceri

Effect of silicate modulus on the setting, mechanical strength and microstructure of iron-rich aluminosilicate (laterite) based-geopolymer cured at room temperature

Cyriaque Rodrigue Kaze, Jean Noel Yankwa Djobo, Achile Nana, Herve Kouamo Tchakoute, Elie Kamseu, Uphie Chinje Melo, Cristina Leonelli, Hubert Rahier

PII: S0272-8842(18)32277-6
DOI: https://doi.org/10.1016/j.ceramint.2018.08.205
Reference: CERI19240

To appear in: *Ceramics International*

Received date: 30 April 2018
Revised date: 17 August 2018
Accepted date: 18 August 2018

Cite this article as: Cyriaque Rodrigue Kaze, Jean Noel Yankwa Djobo, Achile Nana, Herve Kouamo Tchakoute, Elie Kamseu, Uphie Chinje Melo, Cristina Leonelli and Hubert Rahier, Effect of silicate modulus on the setting, mechanical strength and microstructure of iron-rich aluminosilicate (laterite) based-geopolymer cured at room temperature, *Ceramics International,* https://doi.org/10.1016/j.ceramint.2018.08.205

This is a PDF file of an unedited manuscript that has been accepted for publication. As a service to our customers we are providing this early version of the manuscript. The manuscript will undergo copyediting, typesetting, and review of the resulting galley proof before it is published in its final citable form. Please note that during the production process errors may be discovered which could affect the content, and all legal disclaimers that apply to the journal pertain.

ACCEPTED MANUSCRIPT

Effect of silicate modulus on the setting, mechanical strength and microstructure of iron-rich aluminosilicate (laterite) based-geopolymer cured at room temperature

Cyriaque Rodrigue Kaze[a], Jean Noel Yankwa Djobo[b], Achile Nana[e], Herve Kouamo Tchakoute[a], Elie Kamseu[b,c*], Uphie Chinje Melo[a], Cristina Leonelli[c], Hubert Rahier[d]

[a]Laboratory of Applied Inorganic Chemistry, Faculty of Science, University of Yaoundé I, P.O Box 812, Yaoundé, Cameroon.

[b]Laboratory of Materials, Local Materials Promotion Authority, MINRESI/MIPROMALO, P.O. Box 2396, Yaoundé, Cameroon.

[c]Department of Engineering "Enzo Ferrari", University of Modena and Reggio Emilia, ViaP. Vicarelli 10, 41125 Modena, Italy.

[d]Department Materials and Chemistry, Vrije Universiteit Brussel, Pleinlaan 2, 1050 Brussels, Belgium.

[e]Research Unit of Noxious Chemistry and Environmental Engineering, University of Dschang, Faculty of Science, Department of Chemistry, P.O. Box 67, Dschang, Cameroon.

kazerodrigue@gmail.com

chinjeuphie@yahoo.co.uk

Accepted manuscript

ACCEPTED MANUSCRIPT

kamseuelie2001@yahoo.fr

hrahier@vub.be

*Corresponding author. Tel.: 00237222229445; fax: 00237222223720

Abstract

This paper studies the alkali activation of iron-rich aluminosilicates (laterites). Three activating alkaline solutions were prepared from sodium hydroxide solution (8, 10 and 12 M) with sodium silicate (Na_2SiO_3) in order to obtain the sodium silicate solutions with moduli of SiO_2/Na_2O equal to 0.75, 0.92 and 1.04; H_2O/Na_2O=9.78, 10.45 and 12.04. The effects of above-defined solutions on the setting time, physical and microstructural properties of geopolymer binders from calcined laterite (600 °C), containing metakaolinite, as the sole binder at room temperature are reported and discussed. A laterite from Eloumden and one from Odza were used. The synthesized products were labelled $GPEL_{(i=1.04,\ 0.92\ and\ 0.75)}$ and $GPOD_{(i=1.04,\ 0.92\ and\ 0.75)}$ series. The dry compressive strength measured after 7 and 28 days were 4-10 and 10-18 MPa, respectively. It was typically found that the geopolymer paste from sodium hydroxide with molar concentration 12 M and the molar ratio SiO_2/Na_2O of the silicate solution equal to 0.75 produced the highest compressive strength (~ 18 MPa). These samples also have a denser matrix. The dry bulk densities of both series increased with the decrease of silica moduli and were in the range 2.31–2.43 and 2.32–2.52 g/cm^3 and the water absorptions were in the range of 8.21–11.40 % and 7.23-13.03 % for geopolymers GPEL and GPOD series, respectively. The setting time decreased with increasing molarity of NaOH solutions. The physicochemical properties and the mineralogy of both iron-rich

Accepted manuscript

ACCEPTED MANUSCRIPT

aluminosilicates were influenced by the silicate modulus of activating solutions and the best compositions were achieved with characteristic SiO_2/Na_2O=0.75 and H_2O/Na_2O=9.78.

Keywords: laterite, geopolymerization, silicate moduli, compressive strength, microstructure

1. Introduction

Laterite and lateritic soil are reddish or yellowish soils formed in the tropical and subtropical regions of Africa, Australia and South America. They resulted from an alteration of clay via accumulation of iron, Fe^{3+}, or aluminum, Al^{3+}, species [1-4]. In Cameroon, laterite is found on nearly 64% of the national territory [5]. Despite this availability, only a small amount is used successfully as base and sub-base materials in road construction. It is also used for stabilizing earth blocks with Portland cement by the Local Promotion Materials Authority and enterprises of public works. Nevertheless, the mineralogical and chemical compositions of laterites make it suitable for new applications, especially as a cementitious material. The major oxide composition of untreated laterite soils are iron oxide (5–70 wt%), silica (5–70 wt%) and alumina (5–35 wt%), partly present as kaolinite [6-11] allowing it to be considered as raw material for inorganic polymer synthesis. Geopolymers are a class of cementitious materials formed by reaction between an alkaline solution (e.g. sodium or potassium hydroxide and sodium or potassium silicate) and an aluminosilicate source as metakaolin, fly ashes, volcanic scoria etc. Meanwhile most literature deals with metakaolin, fly ash and slags, but much less with volcanic scoria or laterite [12, 13, 14, 15]. Few studies were carried out on alkali activation of laterite, but the properties of the resulting products depend first of all on the chemical and mineralogical composition, composition of activating solution, the physical appearance (like particle distribution and B.E.T specific surface) and the

Accepted manuscript

ACCEPTED MANUSCRIPT

calcination temperature [6-11,16, 17]. As the kaolinite in the laterite is not very reactive, the laterite needs to be calcined to transform kaolinite into metakaolinite. Kaolinite only reacts in the presence of a strong alkaline solution such as a 6 M NaOH solution. This has been extensively studied by M. Esaifan et al. [18, 19]. Even at a temperature of 60 °C it takes several hours for the kaolinite to dissolve and be transformed into a solidified material. For example, Lemougna et al. [9] activated natural laterite, rich in clay mineral (with less than 12wt% of iron oxide) with NaOH at different concentrations and calcined the laterites in presence of NaOH. He found that the compressive strength increases with the increase of NaOH concentration as well as the calcination temperature and the maximum strength was reached after calcination at 450 °C. Afterward Lassinantti Gualtieri et al. [10] prepared geopolymers from laterite (calcined at 700 °C) using both phosphoric acid and alkaline sodium silicate solution, the flexural strength and Young's modulus fell in the ranges 3.3–4.5 MPa and 12–33 GPa, respectively, rendering the materials good candidates for construction purposes. Later, Kaze et al. [11] found that laterite calcination above 500 °C coarsens the particle size, which negatively affects the flexural strength due to a poor polycondensation/polymerization resulting in poor connectivity between the particles. However, Obonyo et al. [8] synthesized geopolymer composites from laterites (adding 15 to 35 wt% of aggregates (river sand) and found that the flexural strengths were in the range 9-13 MPa accompanied with dense microstructure. They concluded that the properties are similar or better compared to fly ash based geopolymer concrete containing 30–60 wt% aggregates (river sand) made by Sofi et al. [12], where the flexural strength values were in the range 4.9–6.2 MPa. Aforementioned authors have used 8 M NaOH solutions as an activator for laterite based geopolymers synthesis. However, no broader study on the strength of laterite based geopolymer and the effect of Na/Si ratio has been reported in literature. The geopolymer properties (chemical and physical) are influenced by SiO_2/Na_2O and H_2O/Na_2O ratios of

Accepted manuscript

ACCEPTED MANUSCRIPT

activating solution. Recent papers of Cristiane et al. [20] and Bignozzi et al. [21] highlight the importance of the above-mentioned oxides ratios, a better comprehension of their influence is envisaged for both calcined laterite (at 600 °C) based geopolymers based on results presented in this paper. So the investigation of the influence of the concentration of sodium hydroxide and the molar ratios SiO_2/Na_2O and H_2O/Na_2O of the alkaline activating solution on some properties of laterite-based geopolymers could be of great interest.

The raw materials used in this project are both calcined laterite at 600 °C harvested from two quarries, have a similar amount of Fe_2O_3, SiO_2 and Al_2O_3 content. Previous work showed that 600 °C is the lower limit for calcining the laterite [11]. The aim of this work was to investigate the best activating solution chemistry, expressed in terms of SiO_2/Na_2O and H_2O/Na_2O molar ratios, for the room temperature activation process in order to tailor the physicochemical characteristics of the iron-rich aluminosilicate binders.

The effect of the moduli of silicate solutions on geopolymerization reaction, and geopolymer structure and physical properties will be studied using setting time (Vicat apparatus), Fourier Transform Infrared Spectroscopy (FTIR), X-ray diffraction (XRD), Scanning Electron Microscopy (SEM/EDS) and evaluation of physical properties (compressive strength, bulk density and water absorption).

The characteristics of laterite based geopolymers are interpreted correlating the silica moduli of activating solution and strength to the microstructure and bulk density. Hence the physicochemical characteristics and mechanical properties of laterite-based geopolymer samples obtained by room temperature alkali activation are reported and discussed to verify their properties in view of their potential applications in building construction materials.

Accepted manuscript

ACCEPTED MANUSCRIPT

2. Materials and Experimental procedures

2.1 Characteristics of Materials used

For this study, the two samples of iron-rich aluminosilicate (laterites) used, were collected in Odza (3°46'60" North and 11°31'60" East) and Eloumden (3°49'0" North and 11°25'60" East), in Yaoundé-Cameroon. After collecting, the raw materials were dried and milled to have fine particles (≤ 80 μm). The resulting powders were calcined at 600 °C during 4 hours (heating/cooling rate of 5 K/min) in a programmable electric furnace and labelled OD600 (from Odza) and EL600 (from Eloumden). This temperature was chosen according to our previous work [11]. The chemical compositions of these starting materials determined by XRF are shown in Table 1. The X-ray patterns (Figure 1) of the calcined materials indicate the presence of anatase (TiO_2, JCPDS N°. 4-447), quartz (SiO_2, JCPDS N°. 5-349); hematite (Fe_2O_3, JCPDS N°. 13-5); ilmenite ($FeTiO_3$, JPDS N°. 3-781); rutile (TiO_2, JCPDS N°. 4-551); boehmite (γ-AlO(OH) N° 21-1307) and corundum (α-Al_2O_3 JCPDS N° 10-173) . Besides these minerals, the calcined material from Eloumden contains maghemite (γ- Fe_2O_3, JCPDS N°. 15-615) (Figure 1b). In addition, the X-ray patterns of EL600 and OD600 show a broad band at 8-30° and 5-27 (2 Theta) respectively (Figures 1a and 1b). These halos are attributed to the presence of a metakaolinite from the transformation of kaolinite. From the simultaneous Differential Thermal Analysis and Thermogravimetric analysis (DSC/TG) carried out in previous work on as-received laterites [11]. The weight loss corresponding to dehydroxylation of OD (laterite from Odza) was 5.01 mass-% and the value for EL (laterite from Eloumden) was 6.24 mass-%. These weight losses correspond to 35.90 and 44.72 % of kaolinite content in laterite from Odza (OD) and Eloumden (EL), respectively. The weak values of weight loss corresponding to the dehydroxylation of kaolinite confirm its alteration due to the replacement of Al^{3+} by iron Fe^{3+}/Fe^{2+} during the laterisation process [3,11] .

Accepted manuscript

ACCEPTED MANUSCRIPT

2.2 Preparation of sodium silicate solutions

The alkaline solutions were prepared from a commercial sodium silicate (14.37 wt% Na_2O, 29.54 wt% SiO_2, 56.09 wt% H_2O) supplied by Ingessil s.r.l. Verona Italy and NaOH pellets (Sigma-Aldrich, purity ≥ 98%). Three aqueous solutions of 8, 10 and 12M were prepared by dissolving NaOH pellets into distilled water and stored at room temperature before their use.

The silicate solutions had molar ratios SiO_2/Na_2O equal to 0.75, 0.92 and 1.04; H_2O/Na_2O=9.78, 10.45 and 12.04. The obtained sodium silicates were allowed to cool down during 12 hours at room temperature prior to use.

2.3 Geopolymer synthesis

The inorganic polymer (geopolymer) samples were formulated by mixing separately calcined laterites to each alkaline solution at a constant liquid/solid ratio of 0.6. The different viscous pastes obtained were poured into cylindrical molds with dimensions 20 (diameter) ×40 (height) cm and sealed into plastic bags in order to prevent water evaporation during the setting and hardening. Then stored at room temperature (25±3 °C) for 24 hours before demolding. The cylindrical specimens were labeled $GPOD_{1.04}$, $GPOD_{0.92}$, and $GPOD_{0.75}$; $GPEL_{1.04}$, $GPEL_{0.92}$ and $GPOD_{0.75}$ for the laterites from Odza and Eloumden, respectively, were used to measure the compressive strength after 7 and 28 days. The indices 1.04, 0.92 and 0.75 represent the molar concentration of sodium silicate solutions.

2.4 Characterization methods of laterite-based geopolymers

The initial and final setting times were measured on the fresh geopolymer pastes using a Vicat needle apparatus according to the EN 196-3 standard. The needle used was 1.00 ± 0.005 mm in diameter.

The compressive strength of the samples was measured with an Instron® 1195 compression machine at 7 and 28 days with a displacement of 5 mm/min according to ASTM

Accepted manuscript

ACCEPTED MANUSCRIPT

C 39. The results shown are an average of four replicate specimens. The strength is given by the equation 1:

$$\delta = \frac{4\times1000\times F}{\pi\times D\times D} \quad (1)$$

With F the force (kN); D the diameter (m) and δ the compressive strength (MPa).

Dry density ρ_d was calculated according to European Standard EN 12390-7. The samples were dried in an oven at 105 °C during several days until stabilization of the mass. The total apparent volume V, dry density (ρ_d) and wet density (ρ_{water}) is then evaluated using following equations, (2) to (4), where M_d: mass dry; $M_{sat:air}$: saturated mass in air (g); $M_{sat:water}$: immersed saturated mass in water (g); $\emptyset_{com}$: apparent porosity (%).

$$V = \frac{M_{sat\ air} - M_{sat\ water}}{\rho_{water}} \quad (2) \qquad \rho_d = \frac{M_d}{V} \quad (3) \qquad \emptyset_{com} = \frac{M_{sat\ air} - M_{sat\ water}}{V}\ x\ 100 \quad (4)$$

The water absorption was carried out by immersing the dried specimens in water at ambient temperature for 24 hours and comparing the humid mass (mh) to the dry mass (md) according to equation 3. The water absorption test was carried out according to ASTM C642-06.

$$Wa = \frac{(mh - md)}{md}\ x\ 100 \quad (5)$$

Infrared Spectroscopy (FT-IR; using an Avatar 330, Thermo Nicolet) was performed on selected samples analyzing surface and bulk areas. A minimum of 32 scans between 4000 and 400 cm^{-1} was averaged for each spectrum with 1 cm^{-1} resolution. The analysis was done on powders from the pieces collected from mechanical testing. For the analysis, each powder sample was mixed with KBr in the proportion of 1/150 (by weight) for 15 min and pressed into a pellet using a hand press.

Accepted manuscript

ACCEPTED MANUSCRIPT

Laterite based geopolymer specimens aged for 28 days were crushed and sieved through a sieve of mesh 80 μm. The powders were subjected to X-ray powder diffractometer (XRD; applying a PW3710, Phillips) using Cu Kα, Ni-filtered radiation (the wavelength was 1.54184 Å). The radiation was generated at 40 mA and 40 kV. Each analysis was performed on fine grains of ground samples. Random powder specimens were step-scanned from 5° to 70°, 2 Theta range, and integrated at the rate of 2s per step. The crystalline phases were identified by comparison with tabulated data on the JCPDS files.

Pieces from the mechanical testing were polished, gold coated and dried for microstructural observations using a JEOL JSM-6500F Scanning Electron Microscope (SEM) coupled with Energy Dispersive X-ray spectroscopy (EDX) with an acceleration voltage of 10.0 kV.

3 Results and discussion

3.1 Effect silicate modulus on laterite-based geopolymer pastes

The results of setting time of the fresh geopolymer pastes are summarized in Table 2. It is observed that the decrease of silicate modulus from 1.04 to 0.75 favoured the shortening of setting time of laterite-based geopolymers. The initial setting times decreased from 107 to 57 min (GPEL) and 124 to 43 min (GPOD). The final setting times were in the range of 135 to 68 (GPEL) and 157 to 86 min (GPOD). A shorter setting time for lower values of silicate modulus (Table 2), was also reported in the literature [22, 23]. It is explained by the increase of the Na_2O concentration which also increases the pH of the alkaline solution resulting in a faster dissolution of calcined laterite. This implies that the building blocks for the polycondensation are quicker available thus accelerate the setting [24, 25]. The trend of initial and final setting is in agreement with previous work [26, 27] which related the faster reaction of other aluminosilicates to the increased concentration of Na^+ in the alkaline solution. The Na/Al molar ratios deduced from each design formulation in both laterite based geopolymer

Accepted manuscript

ACCEPTED MANUSCRIPT

binders are also reported in Table 2. The values were 1.13, 1.27 and 1.44 (for geopolymers $GPOD_{1.04}$, $GPOD_{0.92}$ and $GPOD_{0.75}$, respectively) and 1.16, 1.30 and 1.48 (for geopolymers $GPEL_{1.04}$, $GPEL_{0.92}$ and $GPEL_{0.75}$, respectively). It is noticed that the Na/Al also affected the setting of laterite based geopolymer binders as well as silicate modulus. The shortest setting times were reached with the higher Na/Al ratios of 1.44 and 1.48. Geopolymers from other aluminosilicate precursors, normally have an optimum Na/Al ratio close to one. This Na/Al ratio for the laterite is thus high. This difference is due to the low amount of aluminium content.

3.2 FTIR spectra of laterite-based geopolymers

The infrared spectra of synthesized products are presented in Figures 2 and 3. The broad bands observed in the range 3387–3410 and 1594–1638 cm^{-1} (Figures 2a-3a), 3380–3421 and 1582–1632 cm^{-1} (Figures 2b-3b) correspond to the O–H stretching and H–O–H bending vibration modes. These bands indicate the presence of water molecules, which are surface absorbed or entrapped in the large cavities of polymeric networks. The absorption bands around 1412–1423 cm^{-1} (Figures 2a and 3a) and 1384–1430 cm^{-1} (Figures 2b and 3b) are related to C–O stretching of carbonate groups which are found in all spectra of geopolymer specimens due to the formation of sodium carbonate. A similar reaction was observed by Djobo et al. [28] during geopolymer synthesis from a combination of oyster shell and volcanic ash. The splitting of the peak in the range of 1382–1460 cm^{-1} in all spectra of $GPEL_{(i=1.04,\ 0.92\ and\ 0.75)}$ and $GPOD_{(i=1.04,\ 0.92\ and\ 0.75)}$ samples indicates (Figures 2b and 3b) the elimination of degeneracy due to the distortion of the CO_3^{2-} group, according to Fine and Stolper [29]. They also reported that the degree of splitting depends on the metal ion (Na^+, Ca^{2+} and Mg^{2+}) associated to the carbonate group. A divalent cation linked to the carbonate ion induces a higher energy band in comparison to that of the Na-carbonate. In this work both materials are ferruginous soils, thus the potential cations capable to fix the carbonate are Na^+ and Fe^{3+}/Fe^{2+}.

Accepted manuscript

ACCEPTED MANUSCRIPT

This is likely because some iron minerals might partially take part in the reaction as will be discussed in the XRD section. The degree of splitting of the band is less prominent in the IR spectra of $GPOD_{0.75}$ and $GPEL_{1.04}$ samples. The values of the degree of splitting are 57, 69 and 80 cm^{-1} (for $GPEL_{1.04}$, $GPEL_{0.75}$ and $GPEL_{0.92}$ samples, respectively) and 49, 61 and 63 cm^{-1} (for $GPOD_{0.75}$, $GPOD_{1.04}$ and $GPOD_{0.92}$ specimens, respectively) (Figures 2b and 3b). The lower values of the degree of splitting might indicate a local environment of association between the Na^+ ion with CO_3^{2-} (Na_2CO_3), whereas for geopolymers synthesized with low silica modulus, the high degree of splitting is related to the presence of a Fe-carbonate complex. The higher ones are due to the nature of the iron cation which is divalent/trivalent in comparison to the ion sodium which is monovalent. Since the geopolymer specimens contain iron oxides in their mineralogical composition, this pronounced splitting could likely be linked to the possible beginning of the partial carbonation of non-integrated iron ions in air atmosphere. Then there is the possibility of carbonation of residual iron ions following Eq. (6).

$$Fe^{2+} + CO_3^{2-} \rightarrow FeCO_3$$

The absorption bands situated in the range of 956–1020 cm^{-1} (Figures 2a and 3a) and 975–1015 cm^{-1} (Figures 2b and 3b) were attributed to the asymmetric stretching of Si–O–Fe, Si–O–Al and Si-O-Si bonds in the developing geopolymer network, characteristic peaks of the inorganic polymer network [30, 31, 32]. The smaller broad bands at 475-487 and 568-610 cm^{-1} are attributed to Si-O-T (T=Al, Si, Fe) bending mode, and eventually to Fe-O stretching and deformation vibrations [33, 34]. These bands generally are attributed to T-O bond (T=Al, Si and Fe) deformation vibrations.

3.3 XRD patterns of laterite-based geopolymer cements

Figures 4a-b show the X-ray patterns of laterite-based geopolymer cements. It can be seen that the major crystalline phases such as quartz, ilmenite, anatase, maghemite and rutile

Accepted manuscript

ACCEPTED MANUSCRIPT

remain even after the chemical attack in alkaline media during the geopolymer synthesis. However the peak intensities of iron minerals (ilmenite, maghemite and hematite) have weakly decreased. This indicates that a few fraction of these mineral phases was dissolved into the alkaline solution, thus they could have either partially or totally taken part in the geopolymerization process. In addition, the iron from ilmenite is in Fe^{2+} form and might be oxidized to Fe^{3+} whereas the one from hematite and maghemite is Fe^{3+}, which could be reduced into Fe^{2+} due the alkalinity of the system. Meanwhile, when the intensity of these iron mineral peaks in XRD patterns of all geopolymers decreased, new crystalline phases containing iron such as fayalite (Fe_2SiO_4, JCPDS N°. 34-178) and siderite, ($FeCO_3$, JCPDS N°. 29-696) are formed along with a sodium carbonate based mineral corresponding to thermonatrite (Na_2CO_3, JCPDS N°. 08-0448). These observations indicate that a part of iron phases in both calcined laterites reacted with some silicate phases to form fayalite, and another part which reacted with CO_2 of the air to form siderite. This also corroborates the observation made in FTIR section where the splitting of the carbonate bands was attributed to the carbonation of iron ions. In any case, the oxidation state of iron in the observed minerals is II, thus Fe^{3+}, from hematite and maghemite has been reduced during the reaction (not considered as being part of the network formed) although their intense reflexion peaks exhibited on geopolymer diffractograms. In the same manner Simon et al. [35], Iacobescu et al. [36], Peys et al. [37], and Onisei et al. [38] produced geopolymer binders from iron-rich slag and fayalite slag. These authors found that during alkaline activation, the ^{57}Fe Mössbauer spectroscopy revealed the oxidation of Fe^{2+} from the fayalite slag to Fe^{3+} in the inorganic polymer binder. They concluded that given the iron-rich inorganic polymer, Fe^{2+} could have been also introduced into the polysialate (Si–O–Al) as geopolymer network modifier. The halo peaks observed in XRD patterns of both calcined laterites in the range 8-30° and 5-27° (2 Theta), from EL600 and OD600, respectively in Figure 1, extended from 16 to 40° (2 Theta)

Accepted manuscript

ACCEPTED MANUSCRIPT

in those of geopolymers (Figure 4). In the calcined laterite, this halo is due to metakaolinite. After geopolymerization, an amorphous structure is formed which contributes to the development of the strength of calcined laterite based geopolymers [39, 40]. The observation made with FTIR where the splitting of the carbonate bands was attributed to iron carbonate can thus not be underpinned. The new minerals formed are however not considered as being part of the inorganic polymer network formed as they are not considered being polymers.

3.4 Compressive strength of laterite-based geopolymers

All geopolymer samples were subjected to compressive strength tests after curing for 7 and 28 days, and the results are summarized in Figure 5. For the series $GPEL_{(i=1.04,\ 092\ and\ 0.75)}$, the compressive strengths range from 3.87 to 9.70 MPa (7 days) and 7.87–17.69 MPa (28 days), whereas for the $GPOD_{(i=1.04,\ 0.92\ and\ 0.75),}$ the compressive strengths were in the range of 3.84–9.43 MPa (7 days) and 8.67 to 18.06 MPa (28 days). The concentration of the activating solution thus has an important effect on the mechanical strengths of laterite based geopolymers. The highest strengths were achieved in geopolymers $GPEL_{0.75}$ and $GPOD_{0.75}$, in which the alkaline solution used was a mixture of 12 M sodium hydroxide which was adjusted by the addition of sodium silicate in 1:1 volume ratio of silicate modulus of 0.75. By increasing the activator (NaOH) concentrations, also SiO_2/Na_2O ratio decreased and a higher strength was measured for silicate moduli (Ms=0.92 and 0.75). This trend is consistent with previous studies [22-27, 41] which have shown that the compressive strength increases with the molar concentration of NaOH on other aluminosilicates. Thereby, these observations may be linked to the high degree of hydrolysis and dissolution of silicon, iron and aluminium containing species that polymerize/polycondensate to form geopolymer with high strength. For both calcined laterites at 600 °C, the compressive strengths obtained using silicate modulus (Ms=1.04) were low and almost similar, pointing out insufficient dissolution or activation of calcined laterite at 600 °C at this lower concentration of activator. The small

Accepted manuscript

ACCEPTED MANUSCRIPT

difference in strengths between geopolymer cements made with silicate modulus (Ms=0.75 and 0.92, respectively) is evidence of the relatively lesser influence of activator concentration on starting material. The increase of Na/Al from 1.13 to 1.44 and 1.16 to 1.48 (Table 2) contributed to the improvement of strength. This increase is linked to high HO^- from Na_2O content which favoured more polycondensation by extending the network resulting in a dense and compact structure with less unreacted particles compared to the ones made with Na/Al ratios of 1.13 and 1.16. Although the compressive strengths are lower compared to alkali-activated cements based on other aluminosilicates, they are suitable for non-structural applications where higher strength is not required.

3.5 SEM/EDS images of laterite-based geopolymers

The fracture surfaces of selected geopolymer binders are presented in Figures 6 and 7. $GPEL_{1.04}$ and $GPOD_{1.04}$ (Figure 6) appeared to be coarser, inhomogeneous and contain more unreacted particles compared to $GPEL_{0.75}$ and $GPOD_{0.75}$ (Figure 6). This coarser nature is due to the low alkalinity of the used activator, (in this case 8M NaOH added) and did not promote complete dissolution of the starting material (calcined laterite). However, surfaces of $GPEL_{0.75}$ and $GPOD_{0.75}$ (Figure 6) samples were less inhomogeneous and denser. The use of an activator with a higher Na content enhances the breakdown of the components of calcined laterite (at 600 °C), and extends the geopolymer network which embeds the unreacted particles within the matrix. EDS results (Figure 8) show that the major elements in the alkali-activated binders are Fe, Si, Al and Na (indicated by EDS analysis in Figure 8). This analysis is in line with the possible insertion of an iron atom from iron-rich mineral phases into the geopolymer network as mentioned in previous studies [35, 36, 37, 39, 42,]. Thereby it does not only act as an impurity but it can be incorporated into the structure as found in the literature [43]. The undissolved particles identified on SEM images also contributed to the increase of strength.

Accepted manuscript

ACCEPTED MANUSCRIPT

3.6 Dry density and water absorption of laterite-based geopolymers

The densities and water absorptions at 28 days of laterite based geopolymers are in the range of 2.31–2.43 g/cm^3; 2.32–2.51 g/cm^3; 8.21–11.4 % and 7.23–13.03 %, respectively for $GPEL_{(i=1.04,\ 0.92\ and\ 0.75)}$ and $GPOD_{(i=1.04,\ 0.92\ and\ 0.75)}$ series (Figures 9 and 10). As seen, the dry density increases with the decrease of the silicate modulus. Higher alkali contents (10 and 12M NaOH) with silica modulus 0.92 and 0.75, respectively, in the mixture thus yield higher reactivity with both calcined laterites, resulting in a denser microstructure and less unreacted particles in comparison with those obtained from lower alkali content (silicate modulus equal to 1.04). Thereby, the high value of density from both $GPOD_{0.75}$ and $GPEL_{0.75}$ specimens are linked to a low amount of unreacted metakaolinite particles, more cohesion between different phases and low amount of microcracks and pores within the matrix. The water absorption of resulting products decreased with the increase of Na_2O concentrations (Figure 10). This is due to higher alkalinity which promotes more dissolution of reactive components from calcined laterite (at 600 °C) powders in alkaline media and reduces the formation of voids within the structure. This trend is similar to the studies reported by Thokchom et al. [44] which stated that the compressive strength of specimens increases with the decrease of water absorption and porosity.

Accepted manuscript

Conclusion

Based on the experimental study reported in this paper, it can be concluded that the silicate modulus and Na/Al affect the setting time, compressive strength, bulk density, water absorption and microstructure of calcined laterite based geopolymers. Calcination of these laterites at only 600 °C is proven to be enough for obtaining a solid precursor for alkali activation with reasonable mechanical properties. The activators with highest Na content, thus lowest silicate modulus, resulted in the samples with highest compressive strength. Both

ACCEPTED MANUSCRIPT

laterite based geopolymer materials from silicate solutions with modulus =0.75 showed excellent results, with a compressive strength up to 18.0 MPa after twenty-eight days. This was supported by the SEM/EDS analysis, which shows less unreacted phases and more cohesion and connectivity between different particles within the matrix compared to the samples based on an activating solution with a higher modulus. The density and water absorption obtained were in the range (2.31–2.43 and 2.32–2.51 g/m^3; 8.21–11.4 % and 7.23–13.03 %). A higher alkalinity promotes more complete dissolution of iron, silica and alumina during the geopolymer reaction. Probably some iron was also incorporated into the aluminosilicate network, thus it contributes to the development of the strength of geopolymers. However both laterites used in this work gave acceptable properties for materials for construction. Further studies need to be conducted to find the best mixture design to achieve the highest compressive strength of laterite based geopolymer mortar and concrete.

Accepted manuscript

Acknowledgments

The authors are grateful to Ingessil S.r.l., Verona, Italy, for providing sodium silicate used in this study. This project received the contribution of the Academic of Science for the Third World TWAS through the financement 15-079 RG/CHE/AF/AC_I to Dr. Elie Kamseu.

References

[1] L.T. Alexander, J.C. Cady, Genesis and Hardening of Lateritic Soils, Tech. Bull. 1282, U.S. Dept. Agric, 1962.

ACCEPTED MANUSCRIPT

[2] M.D. Gidigasu, Laterite soil engineering, Development in Geotechnical Engineering, vol. 9, Elsevier Scientific Publishing Company, Amsterdam, Netherlands, 1976.

[3] Trolard, F.; Tardy, Y. A model of Fe^{3+} -Kaolinite, Al^{3+} -Goethite, Al^{3+} -Hematite equilibria in laterites. Clay Mineral. 24 (1989) 1–21.

[4] Kasthurba, A.K.; Santana, M.; Mathews, M.S. Investigation of laterite stones for building purpose from Malabar region, Kerala state, SW India – Part 1: Field studies and profile characterisation. Construction and Building Materials. 21(2007) 73–82.

[5] Mbumbia, L., de Wilmars, A.M., Tirlocq, J. Performance characteristics of lateritic soil bricks fired at low temperatures: a case study of Cameroon. Construction and Building Materials. 14 (2000) 121–131.

[6] NETTERBERG, F. (1985). Pedocretes. Chapter 10 in Brink, A.B.A.(Ed.), Engineering geology of southern Africa, 4, 286-307, Building Publications, Silverton. (CSIR Reprint RR 430).

[7] Kamseu, E., Nzeukou, A., Lemougna P., Billong, N, Melo, U.C., Leonelli, C., 2013. Induration of laterites in the tropical Areas. Assessment for potential structural applications. Interceram. 62(6), 430-437.

[8] Obonyo, E.A.; Kamseu, E., Lemougna, P.N., Tchamba, A.B., Melo, U.C., Leonelli, C. A Sustainable Approach for the Geopolymerization of Natural Iron-Rich Aluminosilicate Materials. Sustainability. 6 (2014) 5535-5553; doi:10.3390/su6095535.

[9] Lemougna, P.N., Balo Madi, A., Kamseu, E., Chinje Melo, U.F., Delplancke, M.P., Rahier, H. Influence of the processing temperature on the compressive strength of Na activated lateritic soil for building applications. Construction and Building Materials. 65 (2014) 60–66.

Accepted manuscript

ACCEPTED MANUSCRIPT

[10] Lassinantti Gualtieri, M., Romagnoli, M., Pollastri, S., Gualtieri, A.F. Inorganic polymers from laterite using activation with phosphoric acid and alkaline sodium silicate solution: mechanical and microstructural properties. Cement Concrete Research. 67 (2015) 259–270.

[11] Kaze R.C, L.M. Beleuk à Moungam, M.L. Fonkwe Djouka, A. Nana, E. Kamseu, U.F Chinje Melo, C. Leonelli. The corrosion of kaolinite by iron minerals and the effects on geopolymerization. Applied Clay Science 138 (2017) 48–62.

[12] Sofi M., J.S.J. van Deventer, P.A. Mendis, G.C. Lukey, Cement. Concrete. Research. 37 (2007) 251–257.

[13] Kamseu, E., Cannio, M., Obonyo, E.A., Tobias, F., Bignozzi, M.C., Sglavo, V.M., Leonelli, C 2014. Metakaolin-based inorganic polymer composite: effects of fine aggregate composition and structure on porosity evolution, microstructure and mechanical properties. Cement Concrete Composite. 53, 258–269.

[14] H.K. Tchakouté, A. Elimbi, E. Yanne, C.N. Djangang, Utilization of volcanic ashes for the production of geopolymers cured at ambient temperature. Cement Concrete Composite. 38 (2013) 75–81, http://dx.doi.org/10.1016/j.cemconcomp.2013.03.010.

[15] Provis JL, Palomo A, Shi C (2015) Advances in understanding alkali-activated materials. Cement Concrete Research. doi:10.1016/j.cemconres.2015.04.013.

[16] Granizo ML, Blanco-Varela MT, Martínez-Ramírez S. Alkali activation of metakaolins: parameters affecting mechanical, structural and microstructural properties. Journal of Material Science. 42 (2007) 2934–2943.

[17] Patrick N. Lemougna, U.F. Chinje Melo, Marie-Paule Delplancke, Hubert Rahier. 2013. Influence of the activating solution composition on the stability and thermo-mechanical

Accepted manuscript

ACCEPTED MANUSCRIPT

properties of inorganic polymers (geopolymers) from volcanic ash. Construction and Building Materials. 48 (2013) 278–286.

[18] Esaifan, Muayad, Hubert Rahier, Ahmed Barhoum, Hani Khoury, Mohammed Hourani, and Jan Wastiels. 2015. Development of Inorganic Polymer by Alkali-Activation of Untreated Kaolinitic Clay: Reaction Stoichiometry, Strength and Dimensional Stability. *Construction and Building Materials* 91. Elsevier Ltd: 251–259. doi:10.1016/j.conbuildmat.2015.04.034.

[19] Esaifan, Muayad, Hani Khoury, Islam Aldabsheh, Hubert Rahier, Mohammed Hourani, and Jan Wastiels. 2016. "Hydrated Lime/Potassium Carbonate as Alkaline Activating Mixture to Produce Kaolinitic Clay Based Inorganic Polymer." *Applied Clay Science* 126: 278–286. doi:10.1016/j.clay.2016.03.026.

[20] Cristiane, Gomes Kelly, G S T Lima, Torres Sandro Marden, D E Barros Silvio, Vasconcelos Igor Frota, and Barbosa Normando Perazzo. 2010. Iron Distribution in Geopolymer with Ferromagnetic Rich Precursor 643: 131–38. doi:10.4028/www.scientific.net/MSF.643.131.

[21] Bignozzi, Maria Chiara, Stefania Manzi, Maria Elia Natali, William D A Rickard, and Arie Van Riessen. 2014. Room Temperature Alkali Activation of Fly Ash: The Effect of Na_2O/SiO_2 Ratio. *Construction and Building Materials*. doi:10.1016/j.conbuildmat.2014.07.062.

[22] Deepak Ravikumar, Sulapha Peethamparan, Narayanan Neithalath. Structure and strength of NaOH activated concretes containing fly ash or GGBFS as the sole binder. Cement & Concrete Composites. 32 (2010) 399–410.

[23] W. Hajjaji, S. Andrejkovicˇová , C. Zanelli , M. Alshaaer, M. Dondi, J.A. Labrincha, F. Rocha. Composition and technological properties of geopolymers based on metakaolin and red mud. Materials and Design. 52 (2013) 648–654.

Accepted manuscript

ACCEPTED MANUSCRIPT

[24] Fernandez-Jimenez, A., Palomo, A., Sobrados, I., Sanz, J., "The Role Played by the Reactive Alumina Content in the Alkaline Activation of Fly Ashes", Microporous and Mesoporous Materials. 91 (2006) 111-119.

[25] Xie, Zhaohui, Xi, Yunping, "Hardening Mechanisms of an Alkaline-Activated Class F Fly Ash". Cement and Concrete Research. 31 (2001) 1245-1249.

[26] Anuj Kumar and Sanjay Kumar. Development of paving blocks from synergistic use of red mud and fly ash using geopolymerization. Construction and Building Materials. 38 (2013) 865–871.

[27] Mary B. Ogundiran, Sanjay Kumar. Synthesis and characterisation of geopolymer from Nigerian Clay. Applied Clay Science. 108 (2015) 173–181.

[28] Jean Noel Yankwa Djobo, Herve Kouamo Tchakoute, Navid Ranjbar, Antoine Elimbi, Leonel Noumbissi Tchadjie and Daniel Njopwouo. Gel Composition and Strength Properties of Alkali-Activated Oyster Shell-Volcanic Ash: Effect of Synthesis Conditions. Journal of American Ceramic Society. (2016)1–8.

[29] G. Fine and E. Stolper, "Dissolved Carbon Dioxide in Basaltic Glasses: Concentrations and Speciation," Earth Planet. Science Letter. 76 [3–4] (1986) 263–78.

[30] Catherine A. Rees, John L. Provis, Grant C. Lukey, and Jannie S. J. van Deventer. Attenuated Total Reflectance Fourier Transform Infrared Analysis of Fly Ash Geopolymer Gel Aging. Langmuir. 23 (2007) 8170-8179.

[31] M. Criado, A. Fernandez-Jimenez, A. Palomo. Alkali activation of fly ash: Effect of the SiO_2/Na_2O ratio Part I: FTIR study. Microporous and Mesoporous Materials 106 (2007) 180–191.

Accepted manuscript

ACCEPTED MANUSCRIPT

[32] W. K. W. Lee and J. S. J. van Deventer. Use of Infrared Spectroscopy to Study Geopolymerization of Heterogeneous Amorphous Aluminosilicates. Langmuir. 19 (2003) 8726-8734

[33] Farrell, D.M., 1972. A Study of the Infrared Absorption in the Oxidation of Magnetite to Maghemite and Hematite: Mines Branch Inv. Rept. 72–18. Dep. Energy Mines Res., Ottawa, Ontario, Canada (44 pp.).

[34] Sidhu, P.S. Transformation of trace element-substituted maghemite to hematite. Clay Clay Miner. 36 (1) (1988) 31–33.

[35] Simon, Sebastian, Gregor J.G. Gluth, Arne Peys, Silviana Onisei, Dipanjan Banerjee, and Yiannis Pontikes. 2018. "The Fate of Iron during the Alkali-Activation of Synthetic (CaO-) FeOx-SiO_2 slags: An Fe K-Edge XANES Study." *Journal of the American Ceramic Society* 101 (5): 2107–2118. doi:10.1111/jace.15354.

[36] Iacobescu, Remus I, Valérie Cappuyns, Tinne Geens, Lubica Kriskova, Silviana Onisei, Peter T Jones, and Yiannis Pontikes. 2017. "The influence of Curing Conditions on the Mechanical Properties and Leaching of Inorganic Polymers Made of Fayalitic Slag" 11 (3): 317–327. doi:10.1007/s11705-017-1622-6.

[37] Peys, Arne, Claire E White, Daniel Olds, Hubert Rahier, Bart Blanpain, and Yiannis Pontikes. 2018. *Molecular Structure of CaO–FeOx–SiO_2 Glassy Slags and Resultant Inorganic Polymer Binders*. doi:10.1111/jace.15880.

[38] Onisei, Silviana, Alexios P Douvalis, Annelies Malfliet, Arne Peys, and Yiannis Pontikes. n.d. *Inorganic Polymers Made of Fayalite Slag: On the Microstructure and Behavior of Fe*. doi:10.1111/ijlh.12426.

[39] Jean Noel Yankwa Djobo, Antoine Elimbi,Herve Kouamo Tchakoute and Sanjay Kumar.2016. Mechanical activation of volcanic ash for geopolymer synthesis: effect on reaction kinetics, gel characteristics, physical and mechanical properties. RSC Advances, 2016, 6, 39106–39117.

Accepted manuscript

ACCEPTED MANUSCRIPT

[40] Sanjay Kumar, Gábor Mucsi, Ferenc Kristály, Péter Pekker. Mechanical activation of fly ash and its influence on micro and nano-structural behaviour of resulting geopolymers. Advanced Powder Technology (2016) in press.http://dx.doi.org/10.1016/j.apt.2016.11.027.

[41] Duxson P, Provis JL, Lukey G C, Mallicoat SW, Kriven WM, van Deventer JSJ. 2005 Understanding the relationship between geopolymer composition, microstructure and mechanical properties. Colloid Surf A – Physicochem Eng Asp 2005; 269:47–58.

[42] Lemougna, P.N., MacKenzie, K.J.D., Jameson, G.N.L., Rahier, H., Chinje Melo, U.F. The role of iron in the formation of inorganic polymers (geopolymers) from volcanic ash: a57 Fe Mössbauer spectroscopy study. Journal of Material Science. 48 (2013) 5280–5286.

[43] Essaidi, N., Samet, B., Baklouti, S., Rossignol, S. The role of hematite in aluminosilicate-cate gels based on metakaolin. Ceramics-Silikáty. 58 (1) (2014) 1–11.

[44] Thokchom, S. Ghosh, P. and Ghosh, S. Effect of Water Absorption, Porosity, and Sorptivity on Durability of Geopolymer Mortars. ARPN Journal of Engineering and Applied Sciences. 4 (2009) 28-32.

Accepted manuscript

Fig 1a. XRD patterns of non-calcined (OD) and calcined (OD600) laterites from Odza Fig 1b. XRD patterns of non-calcined (EL) and calcined (EL600) laterites from Eloumden

Fig 2a and 2b. FTIR spectra of laterite-based geopolymer from Eloumden

Fig 3a and 3b. FTIR spectra of laterite-based geopolymer from Odza

Fig 4. XRD patterns of laterite-based geopolymers GPEL (a) and GPOD (b) series

ACCEPTED MANUSCRIPT

Fig 5a. Compressive strength of 7 days-aged laterite-based geopolymer GPEL and GPOD series Fig 5b. Compressive strength of 28 days-aged laterite-based geopolymer GPEL and GPOD series

Fig 6. SEM micrographs of geopolymers $GPEL_{1.04}$ (A and B) and $GPOD_{1.04}$ (C and D) samples

Fig 7. SEM micrographs of geopolymers $GPEL_{0.75}$ (A and B) and $GPOD_{0.75}$ (C and D) samples

Fig 8. SEM/EDS analysis obtained for the geopolymers $GPEL_{1.04}$ (A) and $GPOD_{1.04}$ (B) samples

Fig 9. Dry bulk density of laterite-based geopolymer GPEL and GPOD series

Fig 10. Water absorption of laterite-based geopolymer GPEL and GPOD series

Accepted manuscript

ACCEPTED MANUSCRIPT

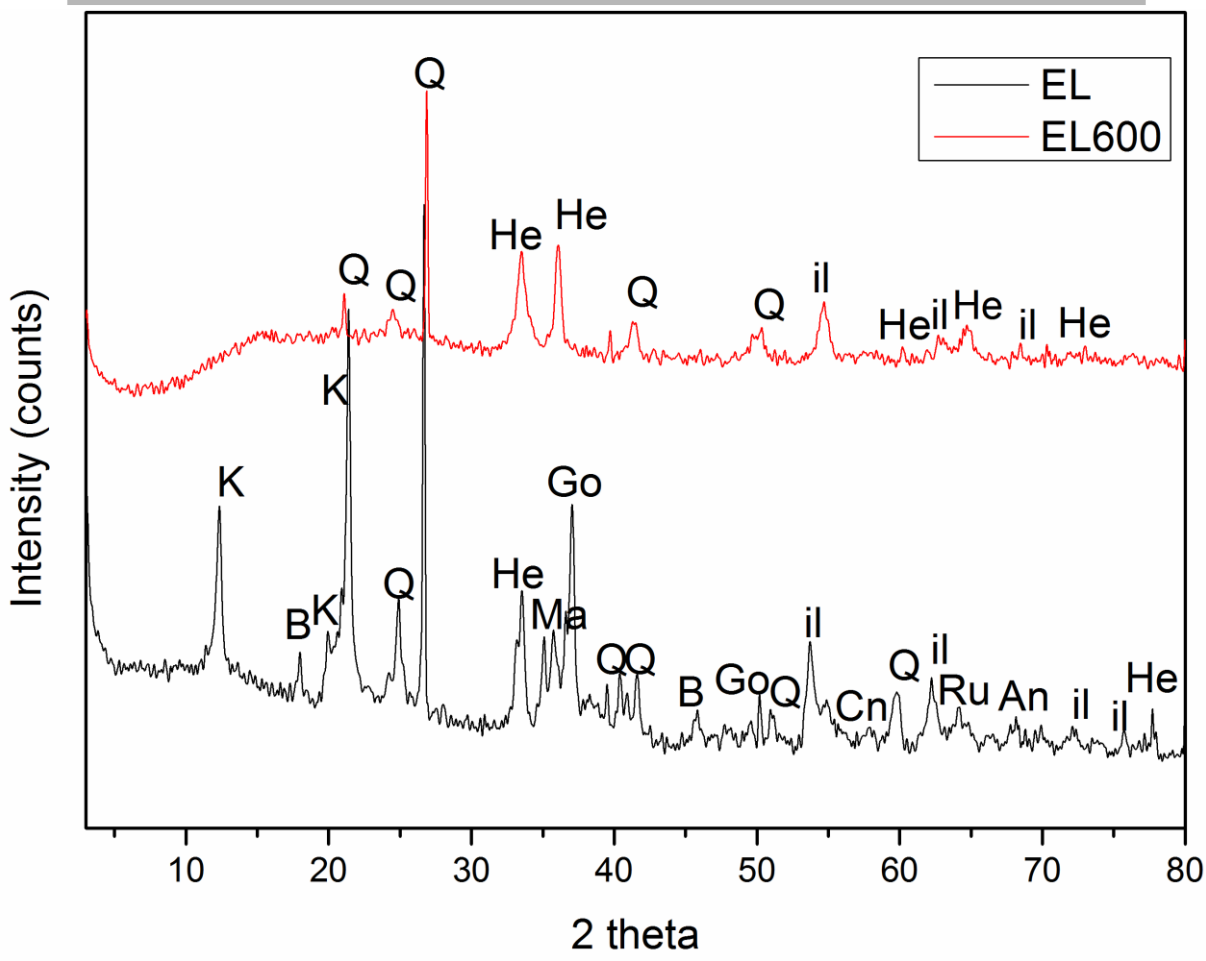

Fig. 1a

Accepted ma

ACCEPTED MANUSCRIPT

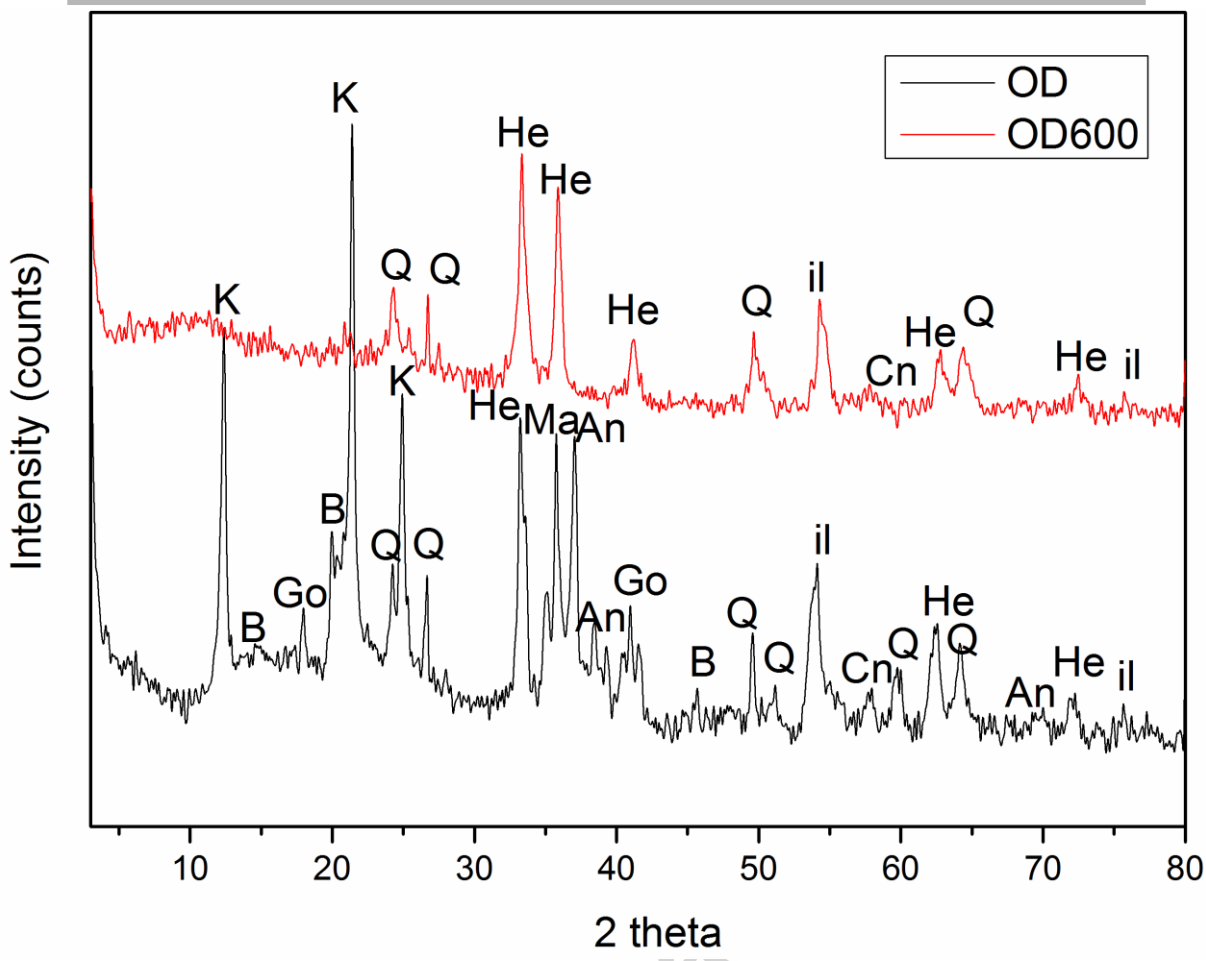

Fig. 1b

Accepted ma

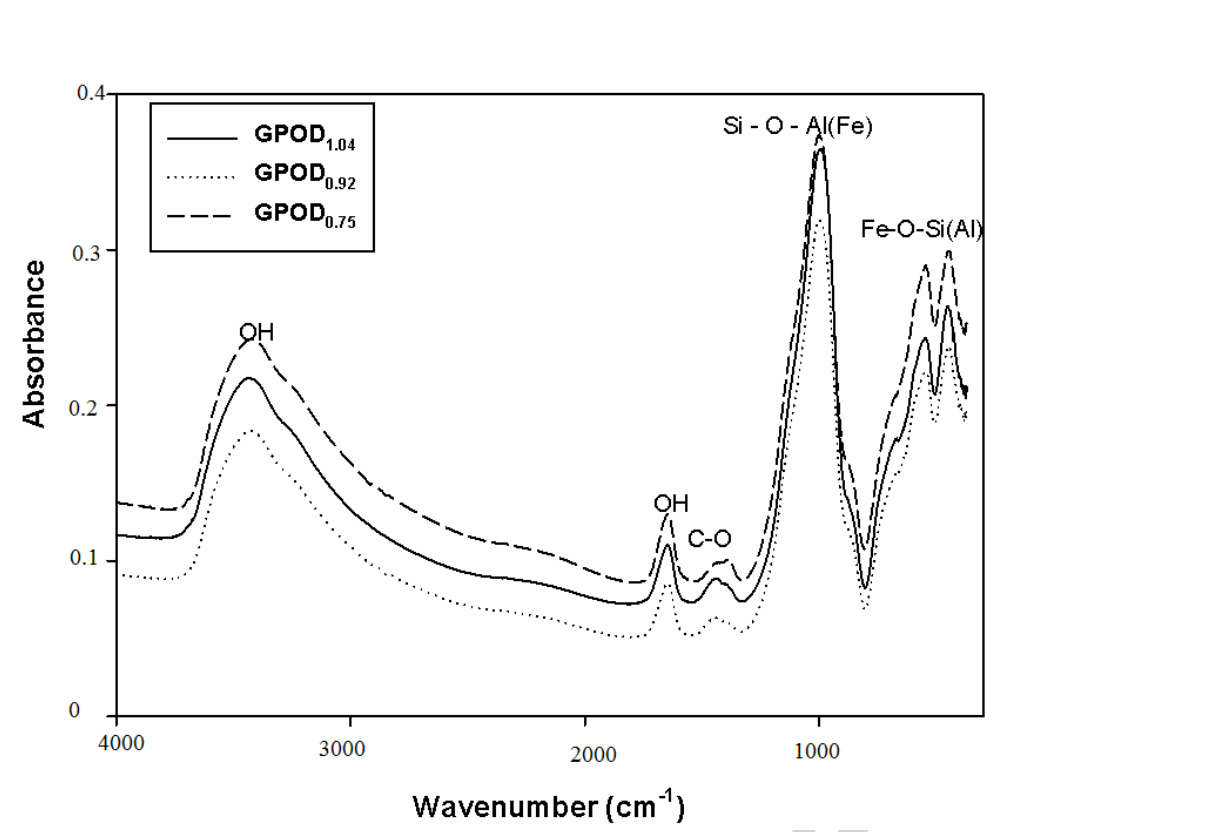

Fig. 2a

Accepted manuscript

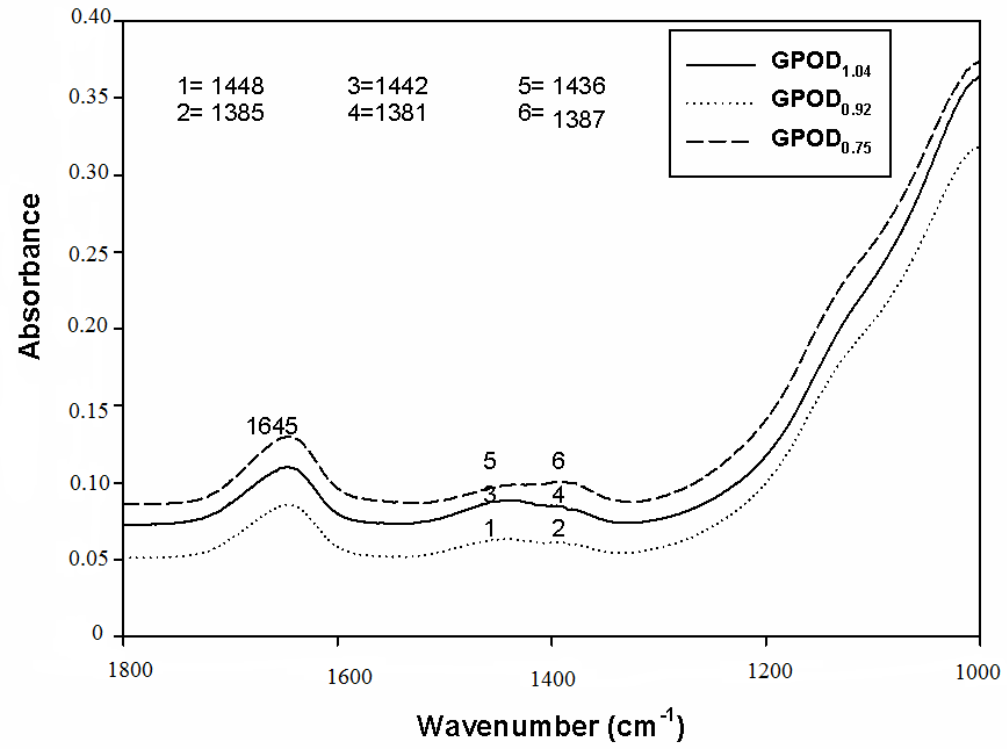

Fig. 2b

Accepted manu-

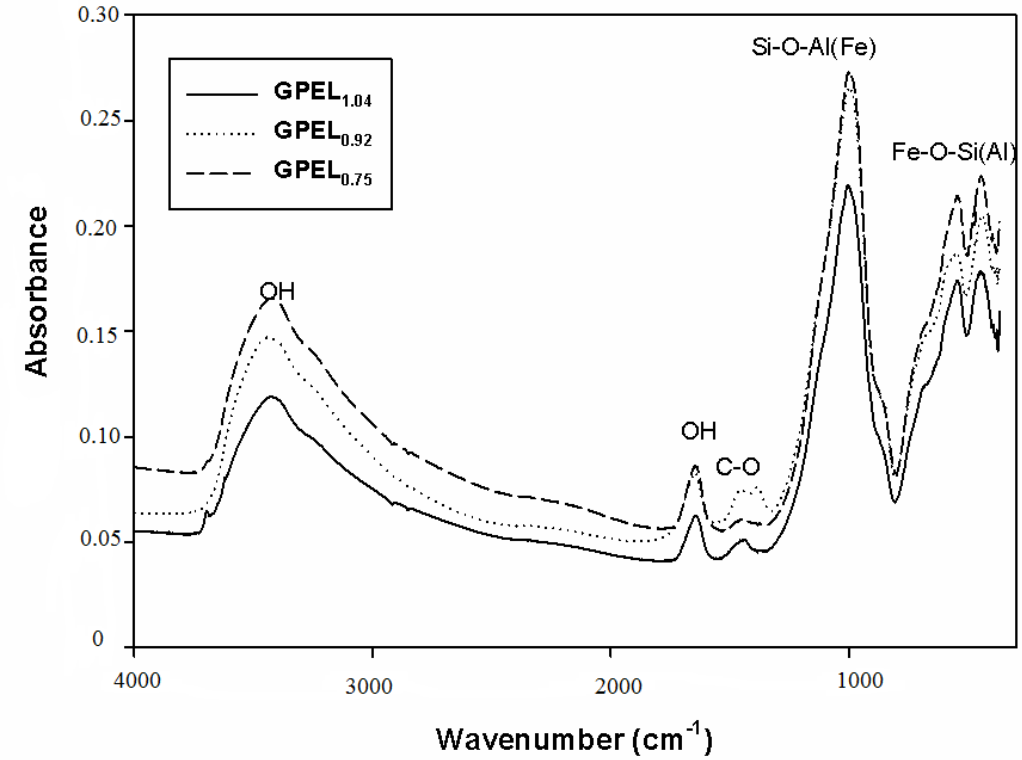
0.30
0.25
0.20
0.15
0.10
0.05
0
Absorbance
GPEL1.04
GPEL0.92
GPEL0.75
Si-O-Al(Fe)
Fe-O-Si(Al)
OH
OH
C-O
4000
3000
2000
1000
Wavenumber (cm-1)

Fig. 3a

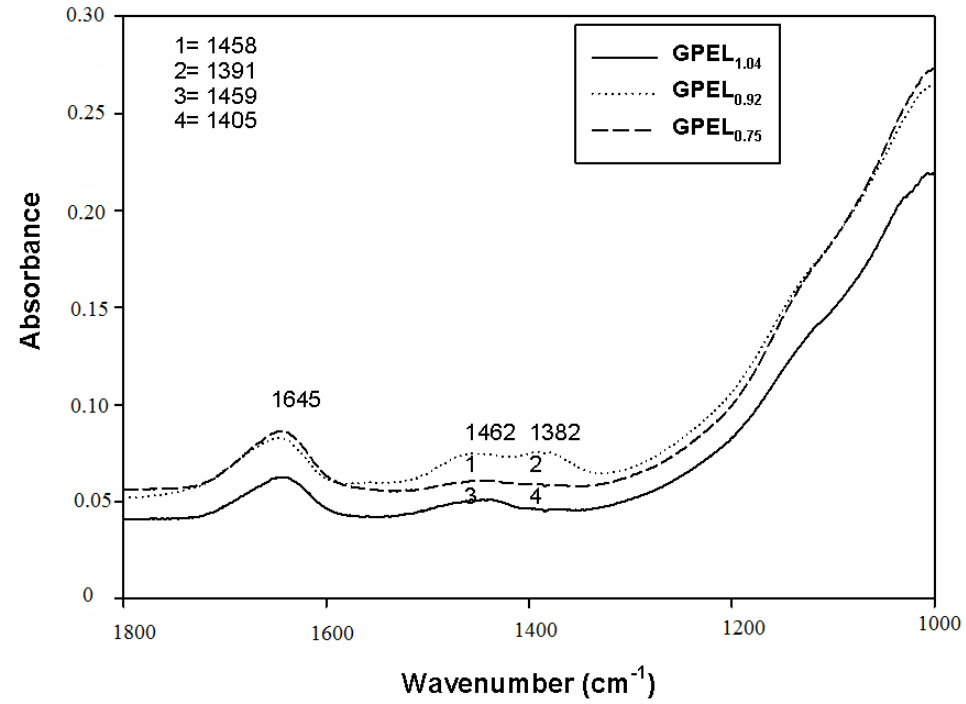
0.30
0.25
0.20
0.15
0.10
0.05
0
Absorbance
1= 1458
2= 1391
3= 1459
4= 1405
GPEL1.04
GPEL0.92
GPEL0.75
1645
1462
1382
1
2
3
4
1800
1600
1400
1200
1000
Wavenumber (cm-1)

Fig. 3b

ACCEPTED MANUSCRIPT

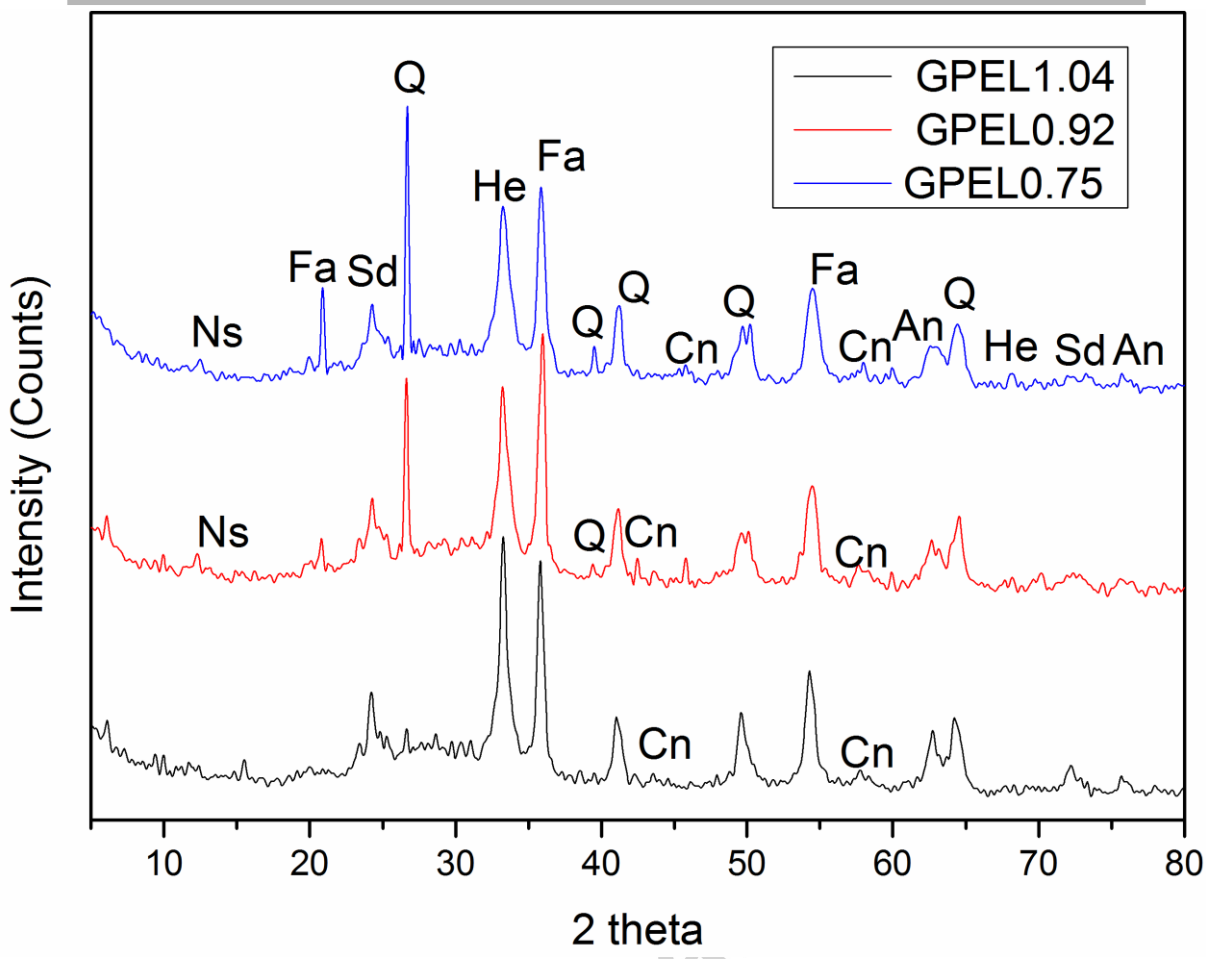

Fig. 4a

Accepted ma

ACCEPTED MANUSCRIPT

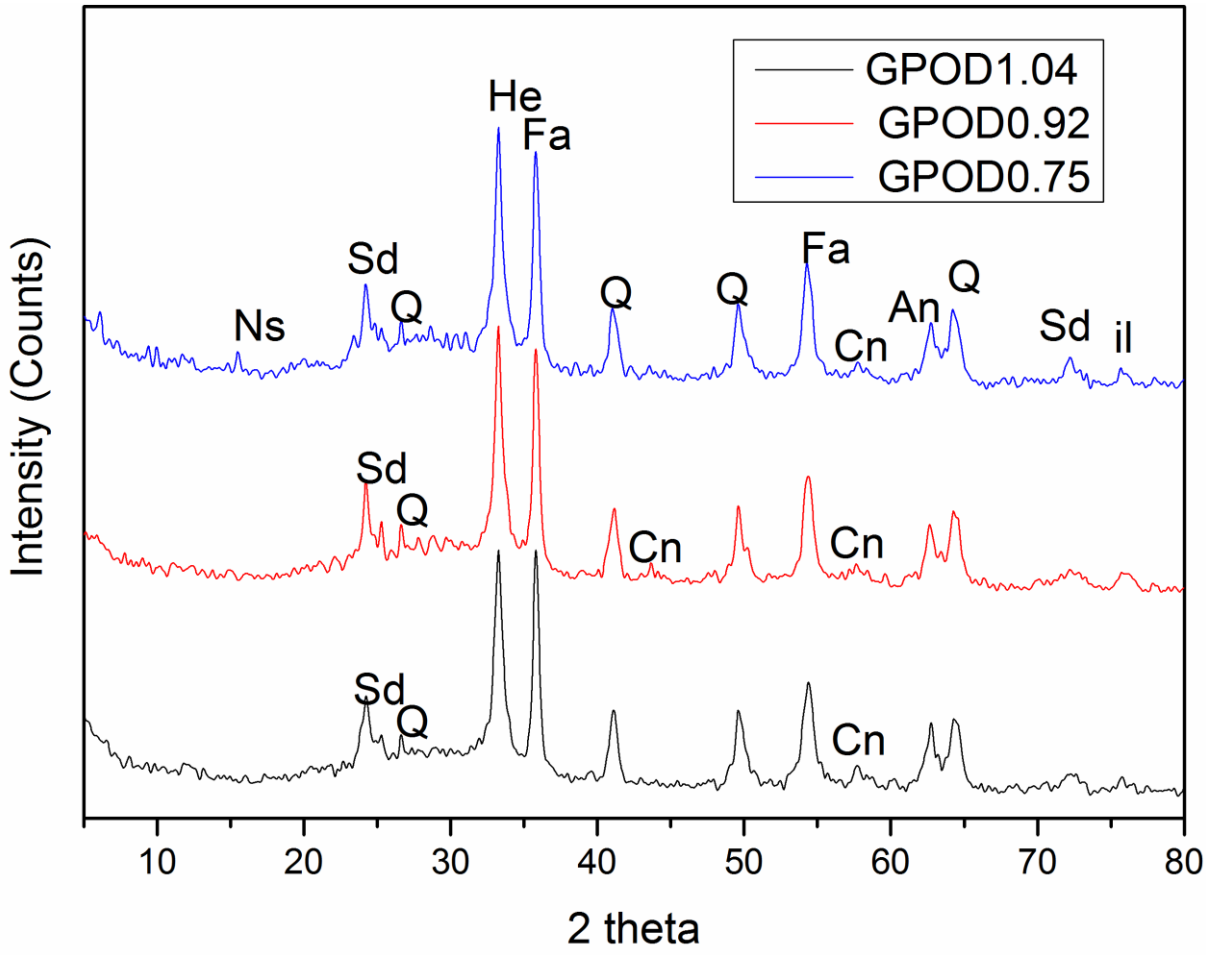

Fig. 4b

Accepted ma

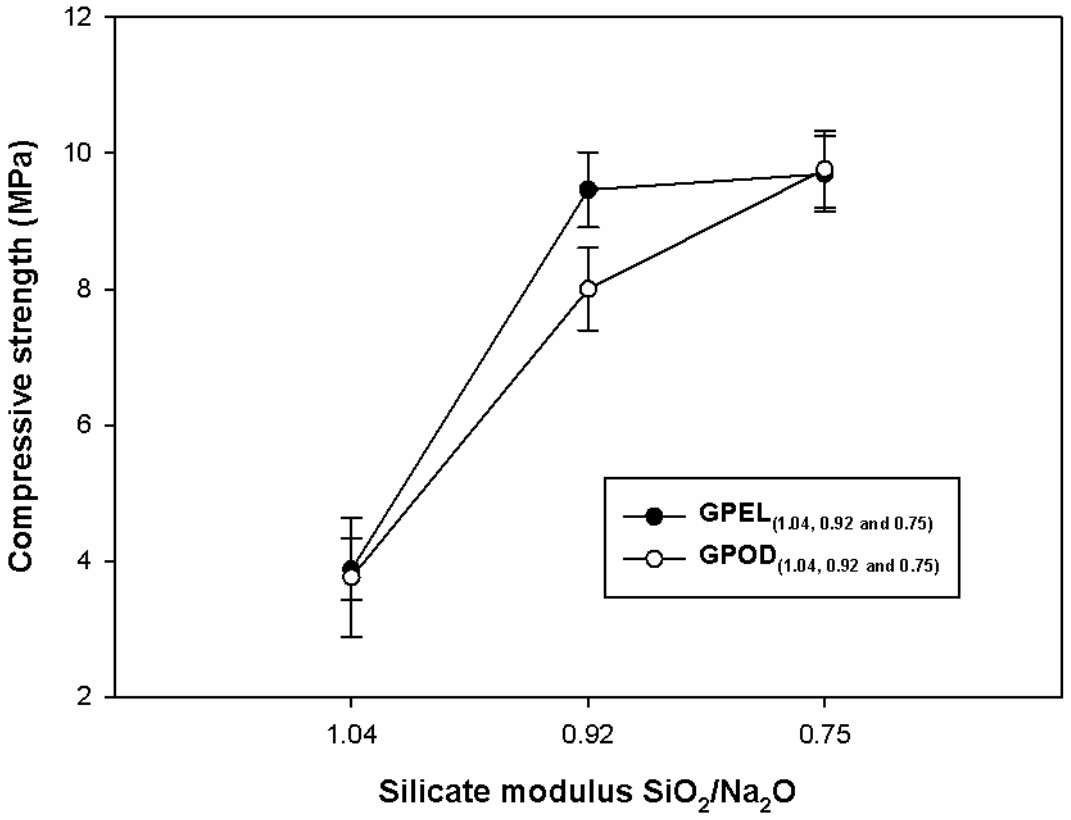

Fig. 5a

Accepted manuscript

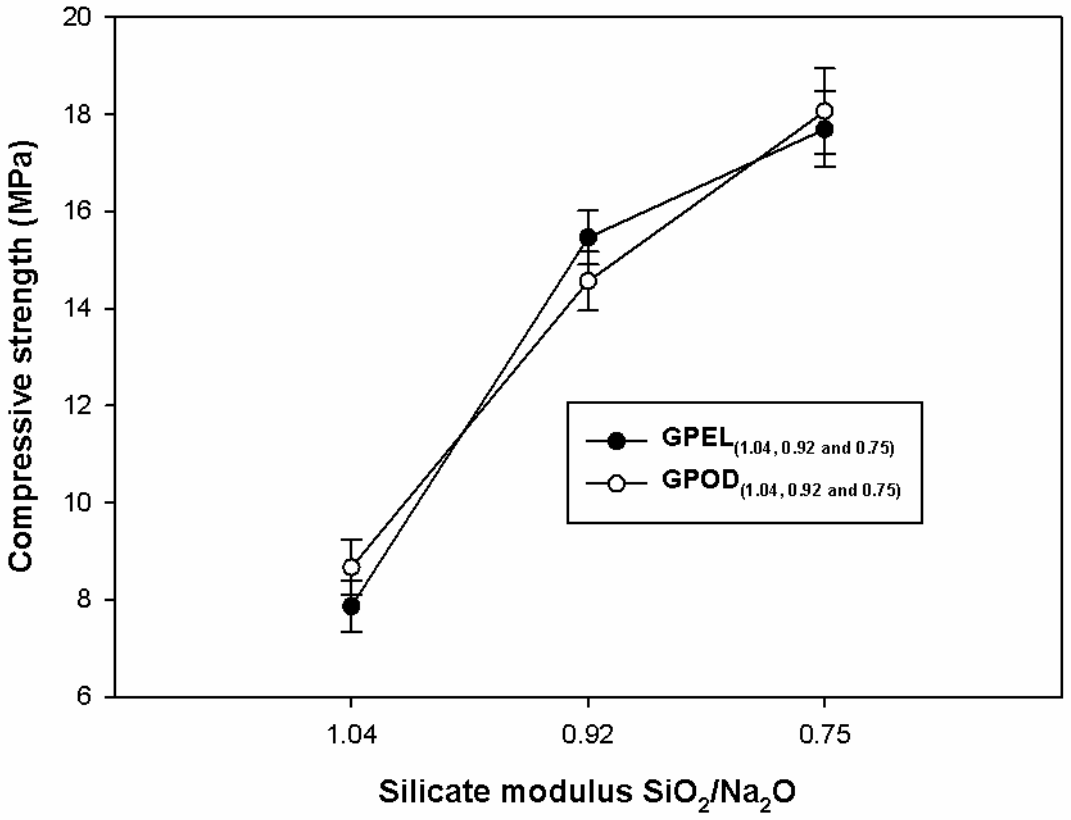

Fig. 5b

Accepted manuscript

ACCEPTED MANUSCRIPT

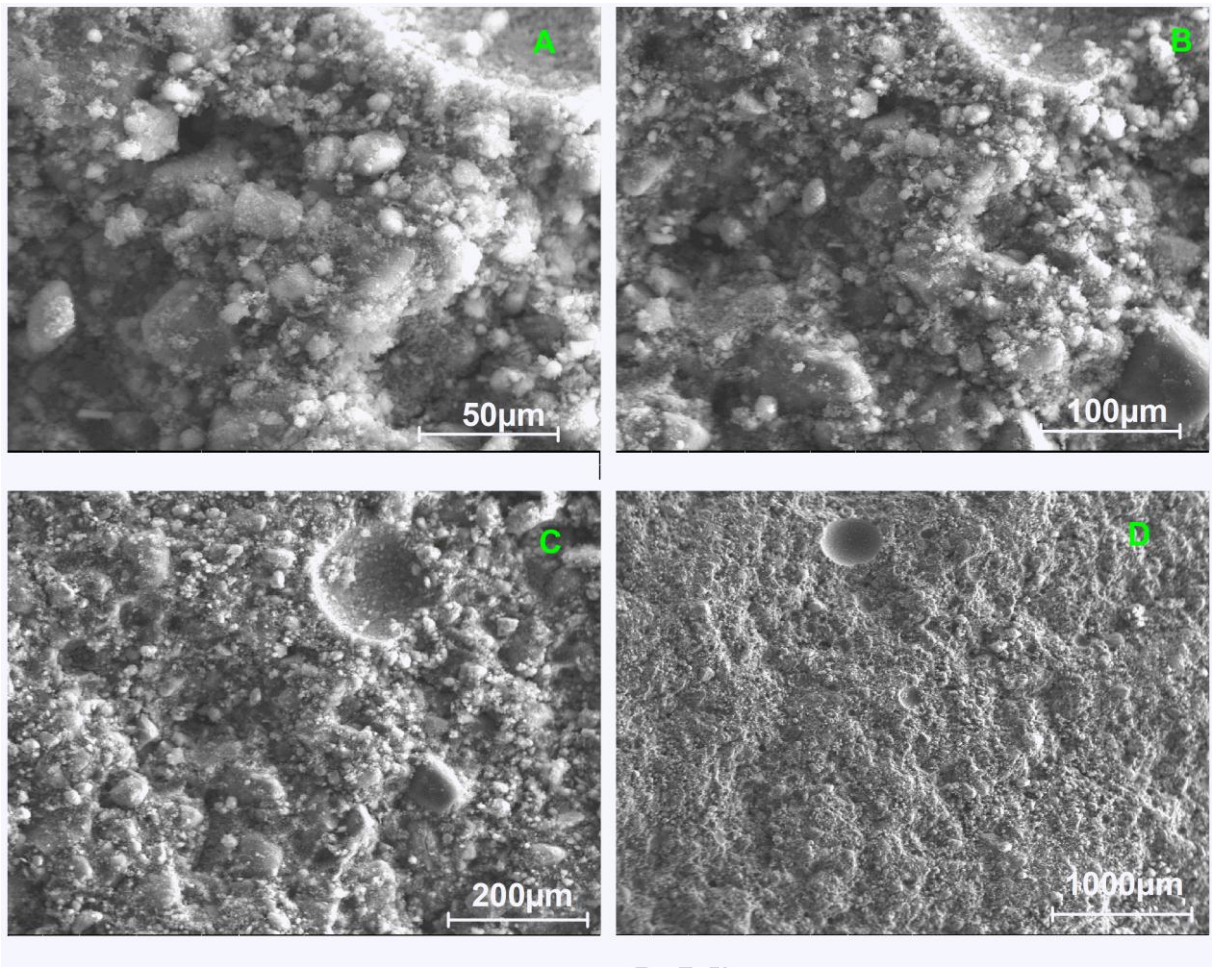

Fig. 6

Accepted ma

ACCEPTED MANUSCRIPT

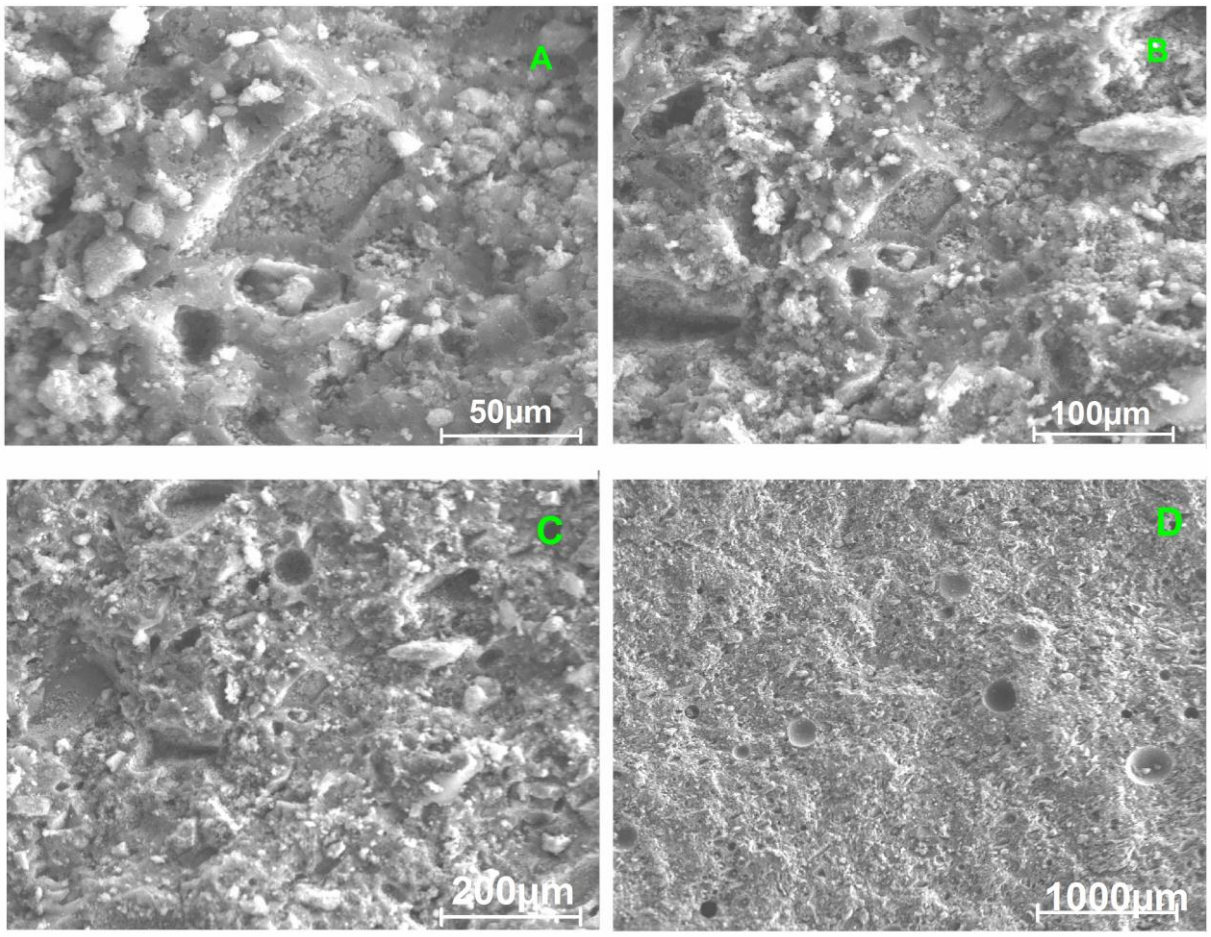

Fig. 7

Accepted ma

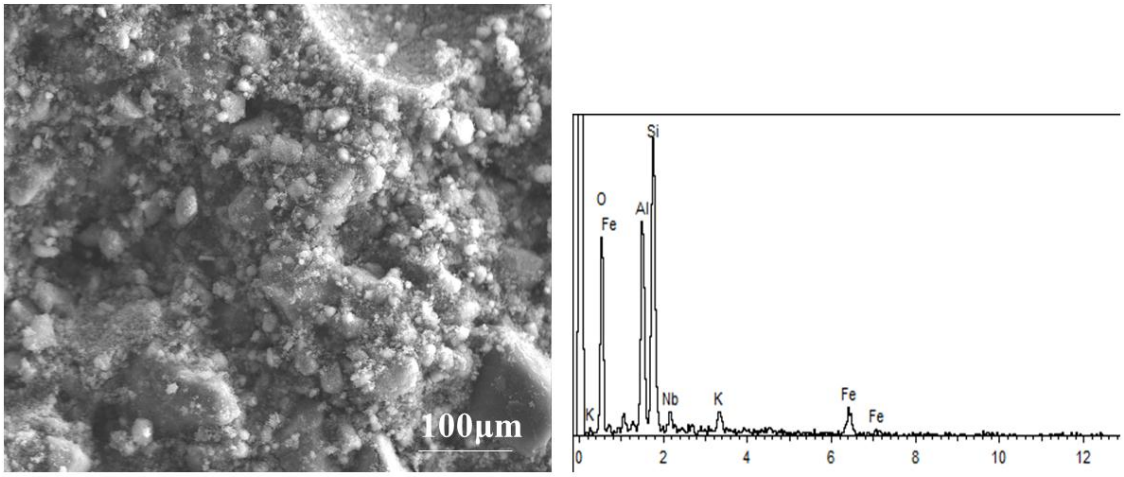
100µm
O
Fe
Al
Si
K
Nb
K
Fe
Fe
0
2
4
6
8
10
12

Fig. 8a

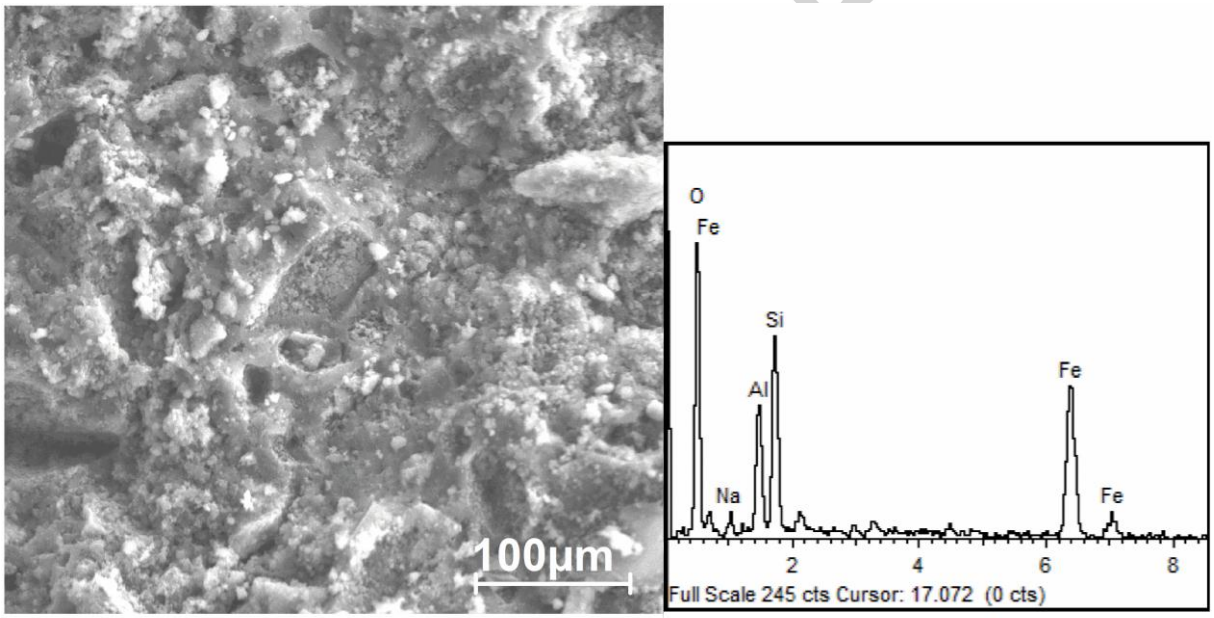
100µm
O
Fe
Si
Al
Na
Fe
Fe
2
4
6
8
Full Scale 245 cts Cursor: 17.072 (0 cts)

Fig. 8b

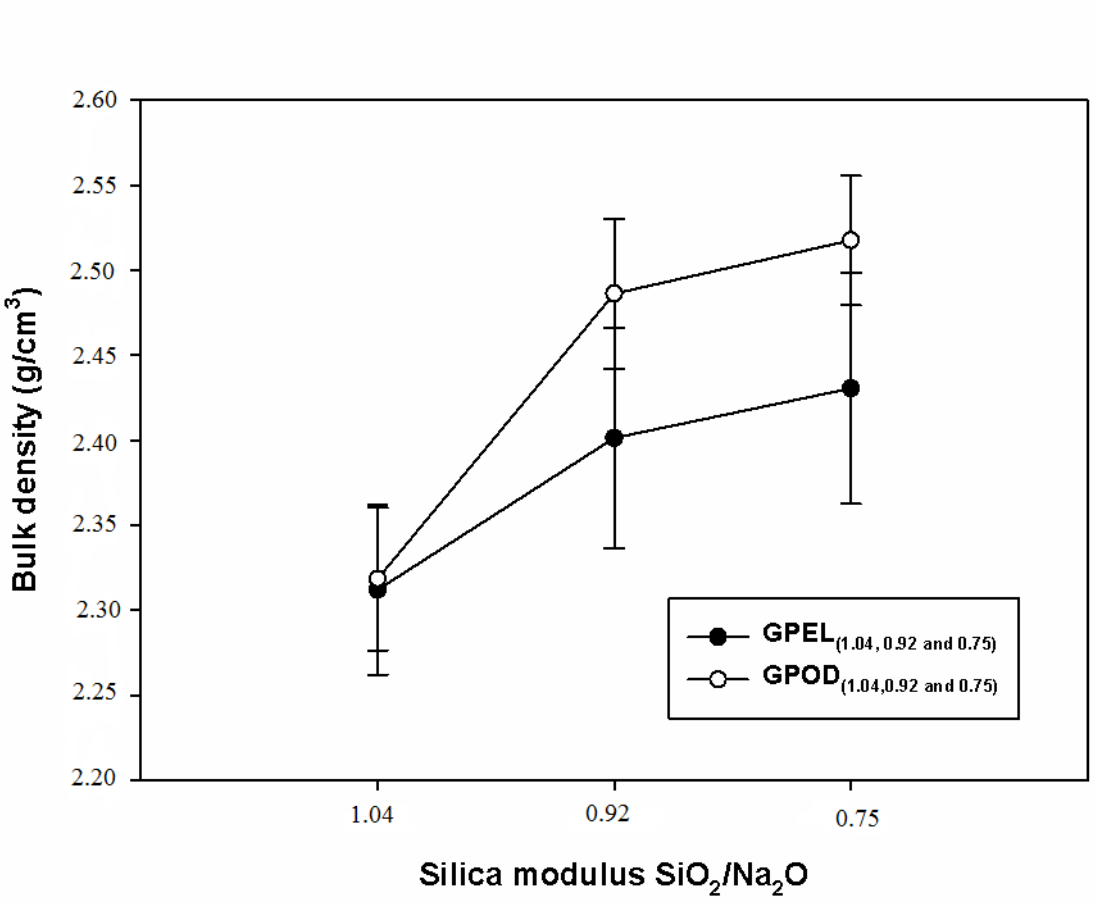

Fig. 9

Accepted manuscript

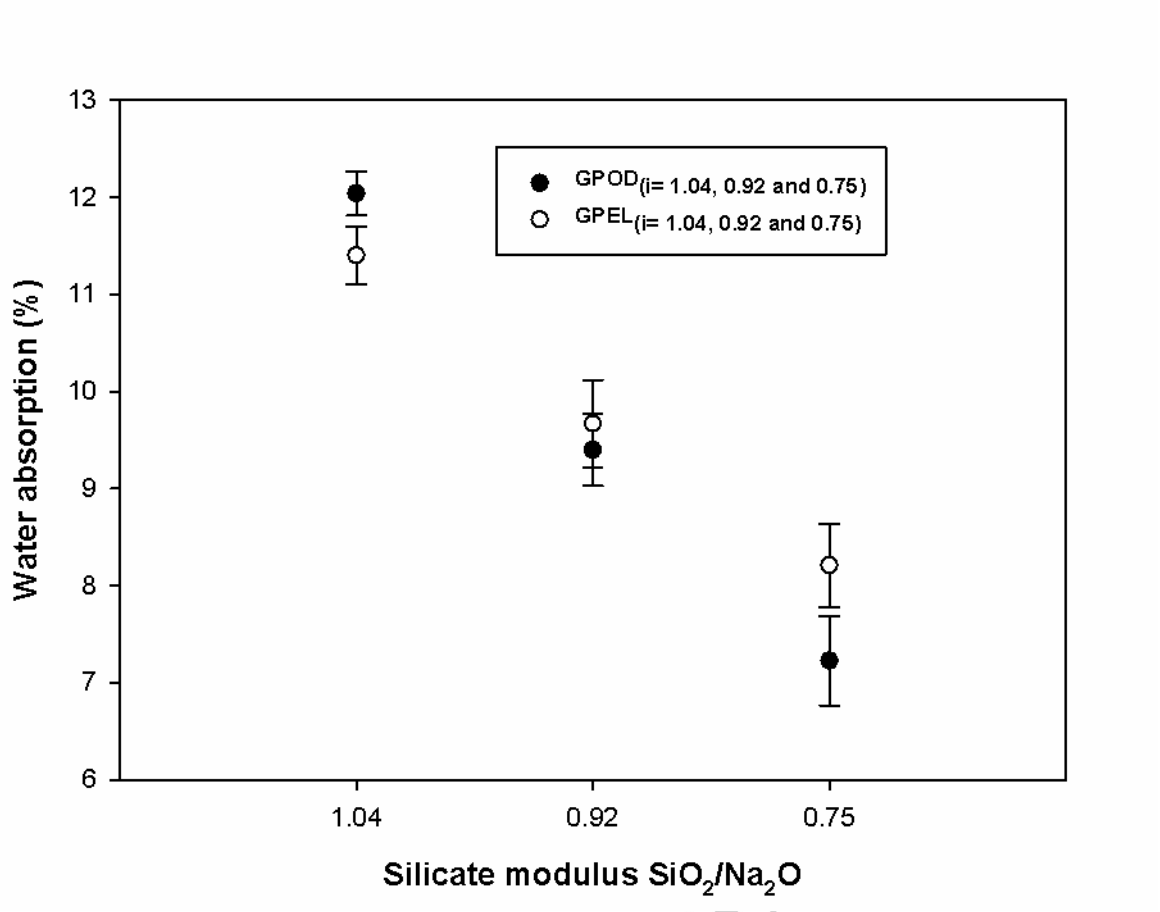

Fig. 10

Table1. Chemical composition of calcined laterite from Eloumden and Odza

Oxides (%)	Fe_2O_3	SiO_2	Al_2O_3	TiO_2	V_2O_5	P_2O_5	L.O.I
EL600	39.00	28.04	25.10	0.23	0.14	0.04	0.95
OD600	38.50	29.40	27.05	0.34	0.17	0.03	1.02

Accepted manuscript

ACCEPTED MANUSCRIPT

Table 2. Setting time (Vicat) of laterite based geopolymers

Geopolymer samples	Initial setting (min.)	Final setting (min.)	Molarity of NaOH solution used	Silicate Moduli SiO_2/Na_2O	H_2O/Na_2O molar ratio	Na/Al molar ratio
$GPEL_{1.04}$	107	135	8	1.04	12.04	1.16
$GPEL_{0.92}$	76	102	10	0.92	10.45	1.30
$GPEL_{0.75}$	57	68	12	0.75	9.78	1.48
$GPOD_{1.04}$	124	157	8	1.04	12.04	1.13
$GPOD_{0.92}$	64	120	10	0.92	10.45	1.27
$GPOD_{0.75}$	43	86	12	0.75	9.78	1.44

Accepted manuscript